MONTANA BUREAU OF MINES AND GEOLOGY
A Department of Montana Technological University

MBMG Geologic Map 101; Plate 1 of 1
Geologic Map of the Beaverhead Rock SE 7.5′ Quadrangle, 2024

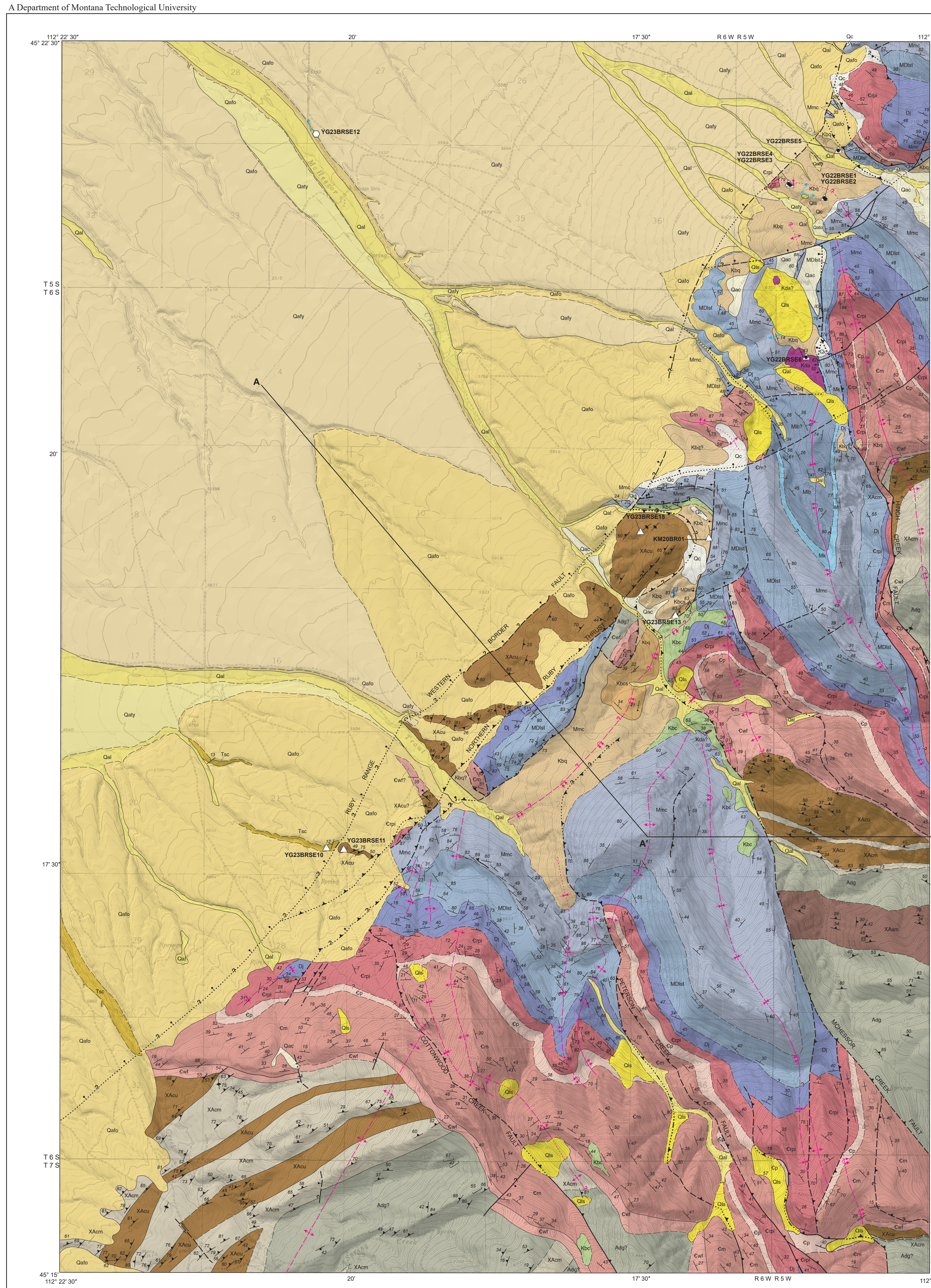

Basemap produced by the United States Geological Survey
Beaverhead Rock SE 1:24,000-scale quadrangle map
Color: by USGS and USC&GC
Compiled from aerial photographs taken 1960
Field checked: 1961
Projection: Polyconic
Vertical Datum: National Geodetic Vertical Datum of 1929
Horizontal Datum: 1927 North American Datum

Shaded relief created from 10-meter digital elevation model from U.S. Geological Survey National Elevation Dataset.

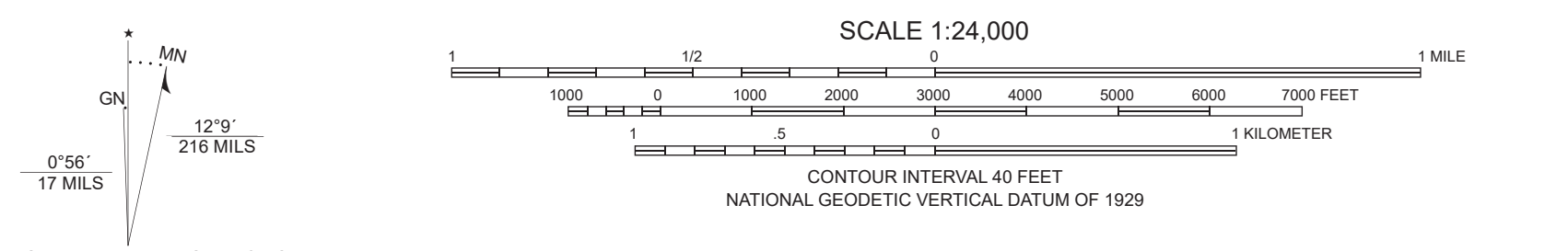

Maps may be obtained from:
Publications Office
Montana Bureau of Mines and Geology
1300 West Park Street
Butte, Montana 59701-8997
Phone: (406) 496-4174
http://mbmg.mtech.edu

Cross Section A–A′–A″

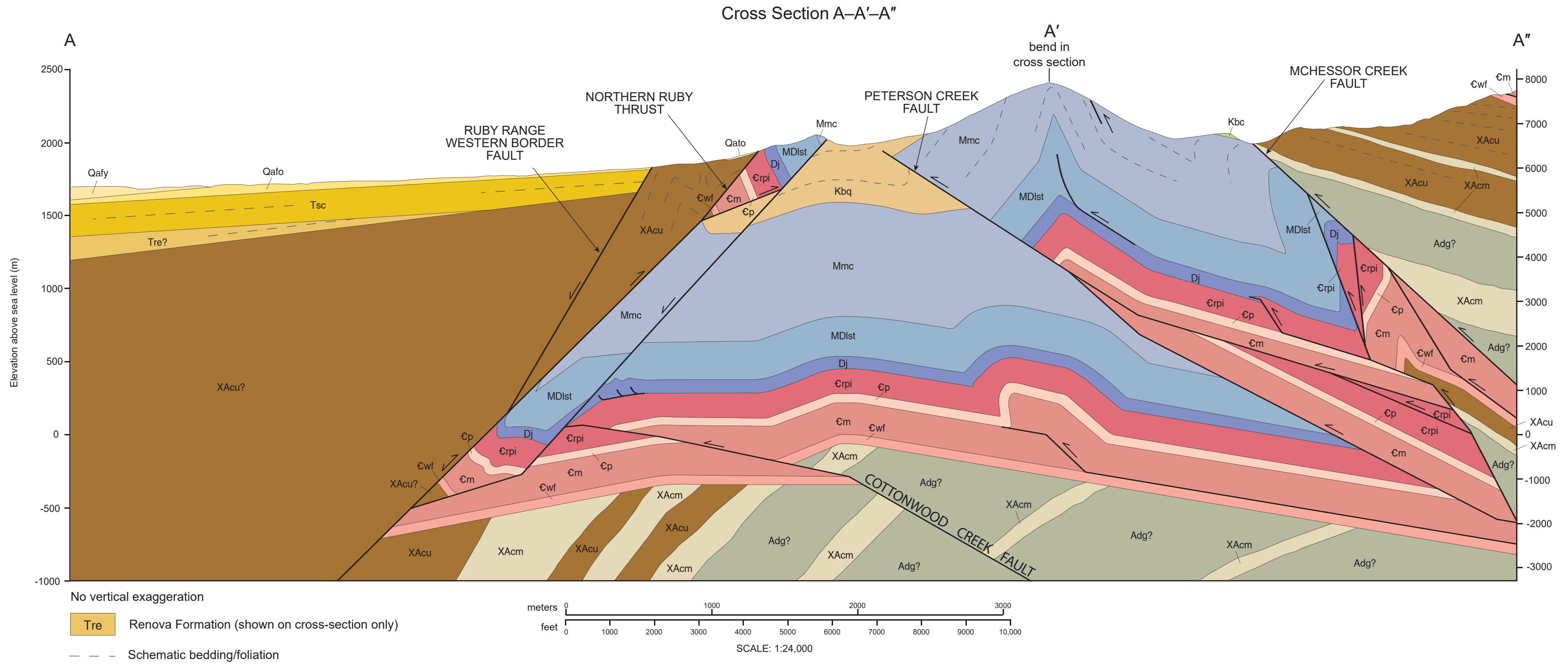

No vertical exaggeration

Tre Renova Formation (shown on cross-section only)

Schematic bedding/foliation

SCALE 1:24,000

CORRELATION DIAGRAM

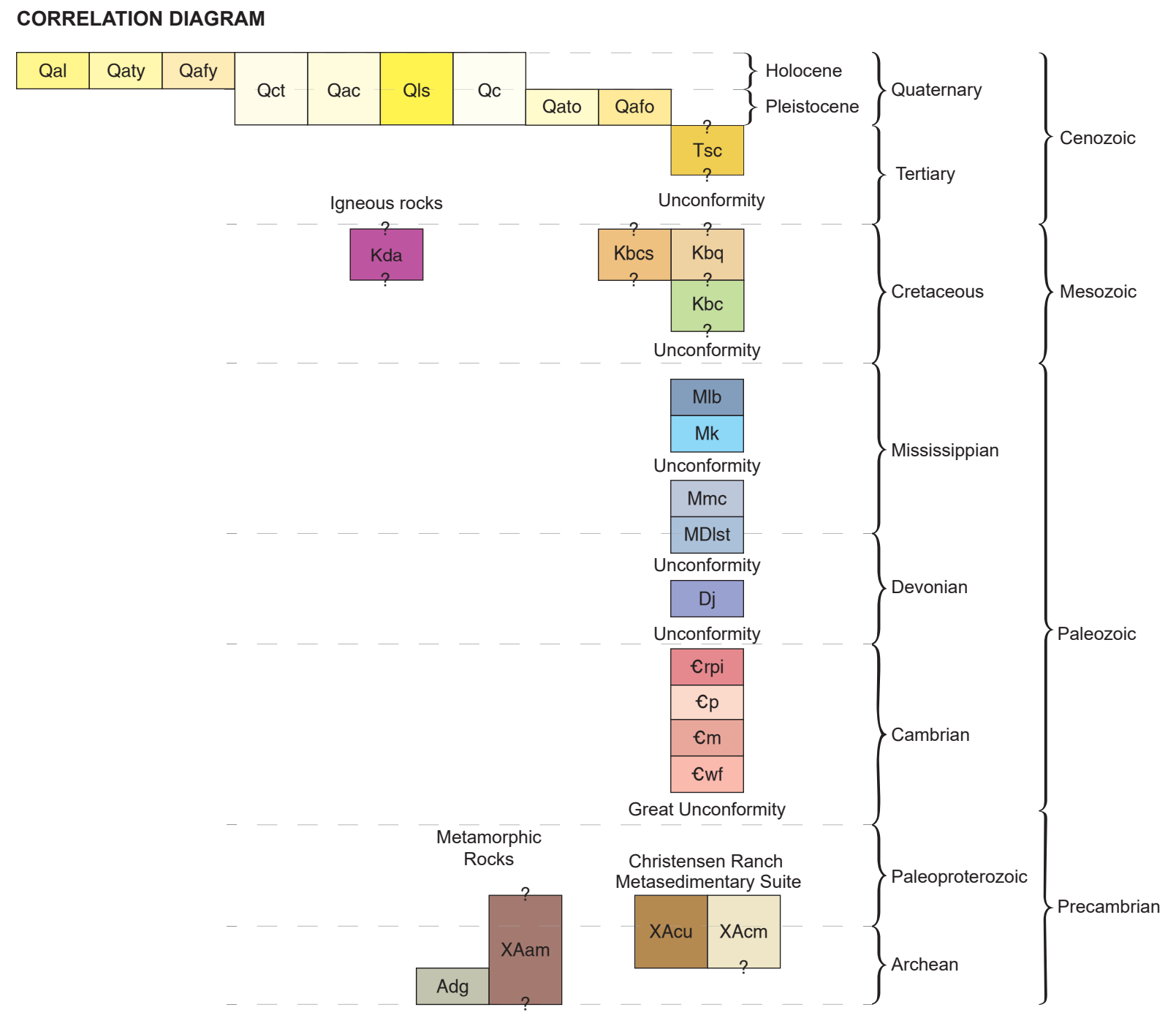

MAP SYMBOLS

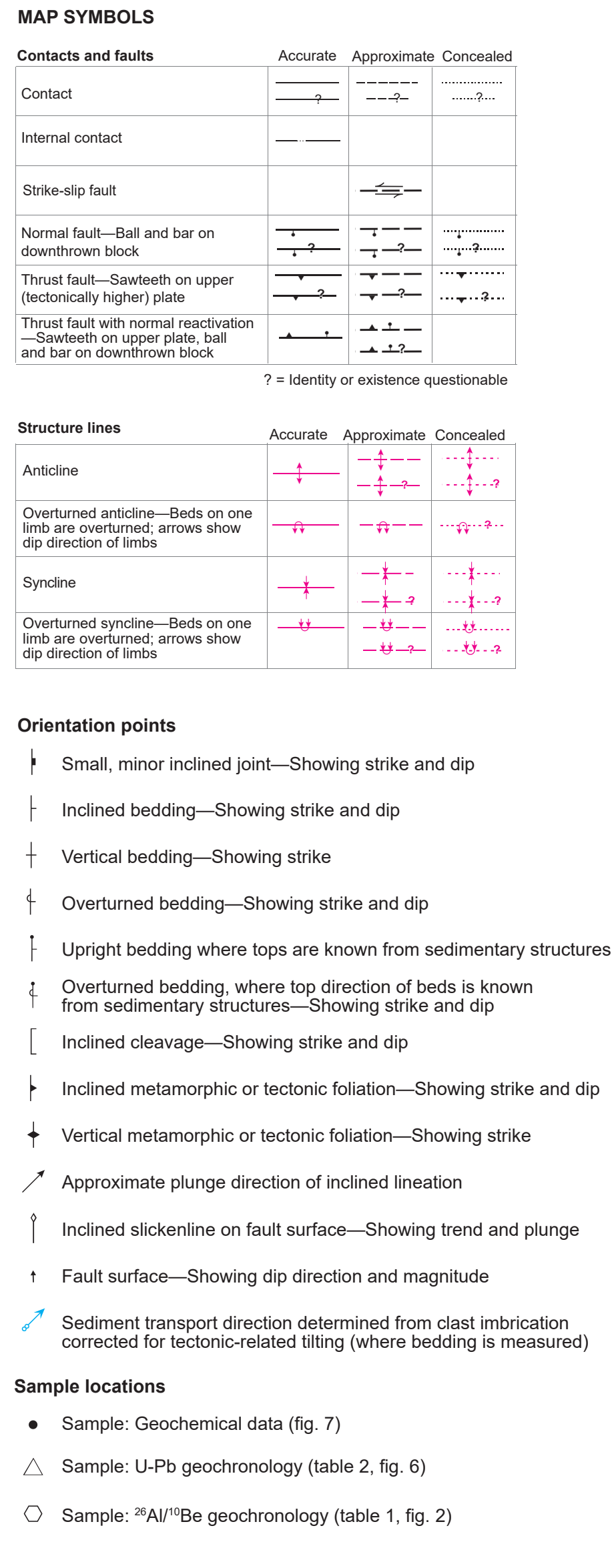

Sample locations

- ● Sample: Geochemical data (fig. 7)
- △ Sample: U-Pb geochronology (table 2, fig. 6)
- ⬡ Sample: ^{26}Al/^{10}Be geochronology (table 1, fig. 2)

INTRODUCTION

The Beaverhead Rock SE 7.5′ quadrangle encompasses the northern part of the Ruby Range, in Madison County, Montana (fig. 1). Much of the mountainous terrain within the quadrangle is part of the Ruby Mountains Wilderness Study Area, with elevations ranging from 8,336 ft (2,541 m) to 5,170 ft (1,576 m). The quadrangle mainly consists of Paleozoic carbonate and Precambrian basement rocks that generally support lush wooded slopes, and various sequences of Quaternary- to Cretaceous-aged gravels that underlay broad surfaces and dry prairie slopes along the range front. Northwest-flowing drainages dissect the northwest Ruby Range, flowing to the Beaverhead River in the valley. Drainages are often parallel to axes of broken southwest-verging folds and are incised within broad alluvial fan deposits. Scarps associated with normal faulting along the northern section of the range front (fig. 1) attest that the Ruby Range western border fault is a Quaternary fault with earthquake potential. A major historic earthquake in 1897, with an estimated intensity magnitude of 5.6 (± 0.4), occurred near the northern Ruby Range (Stickney, 2022), although the exact epicenter location is poorly constrained. While the range front further south exhibits minimal normal faulting at the surface, recent fault displacement and active seismicity may be distributed on blind structures across the Beaverhead Graben, similar to the hypocenter of the 2005 Mw 5.6 Dillon earthquake (Stickney, 2022).

PREVIOUS MAPPING AND METHODS

Tysdal (1970, 1976) mapped the quadrangle at 1:24,000 scale, focusing on the Cambrian stratigraphy. Karasevich (1980) and Karasevich and others (1981) mapped the Precambrian basement in more detail (1:24,000 scale), describing multiple generations of ductile folding. Mapping of mineral resource potential, particularly talc, was conducted by the United States Geological Survey (USGS) as part of their assessment of the proposed Ruby Mountains Wilderness Study Area (Tysdal and others, 1987, 1:24,000 scale). Several structural studies (e.g., Karasevich and others, 1981; Tysdal, 1981; Schmidt and Garihan, 1983; Schmidt and others, 1988) used published maps of the northern Ruby Range in studies of regional tectonics. The Beaverhead Rock SE 7.5′ quadrangle has been included in two regional-scale maps (Ruppel and others, 1983, 1993; scale 1:250,000).

Rock samples collected for U-Pb geochronology were processed at the MBMG mineral separation laboratory. Zircon was isolated from selected samples by standard density and magnetic separation techniques. Zircon separates were analyzed by laser ablation inductively coupled plasma mass spectrometry (LA-ICP-MS) by Jesse Mosolf, Daniel Brennan, and Stuart Parker, MBMG, at the University of California, Santa Barbara. Samples collected for ^{26}Al/^{10}Be cosmogenic nuclide burial dating were physically processed at the MBMG mineral separation laboratory. Quartz was isolated from selected cobble samples using standard separation techniques for cosmogenic nuclides dating. Quartz separates were sent to the Center for Accelerator Mass Spectrometry (CAMS), Lawrence Livermore National Lab for further quartz purification, chemical analyses and measurements of ^{26}Al and ^{10}Be concentrations via accelerator mass spectrometry (AMS). All sample data and age results are shown in tables 1 and 2 (Gavillot and Hidy, in prep.; Mosolf and others, 2023a; Brennan and others, in prep.).

Location Map

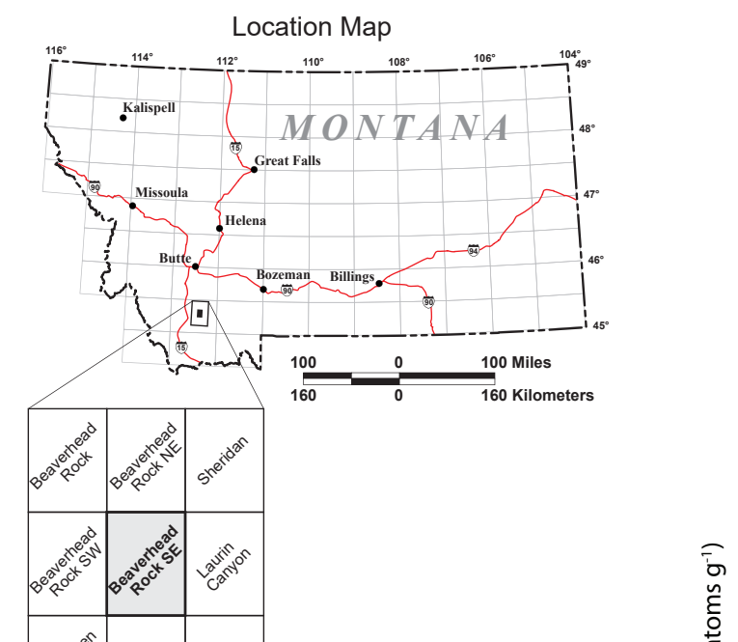

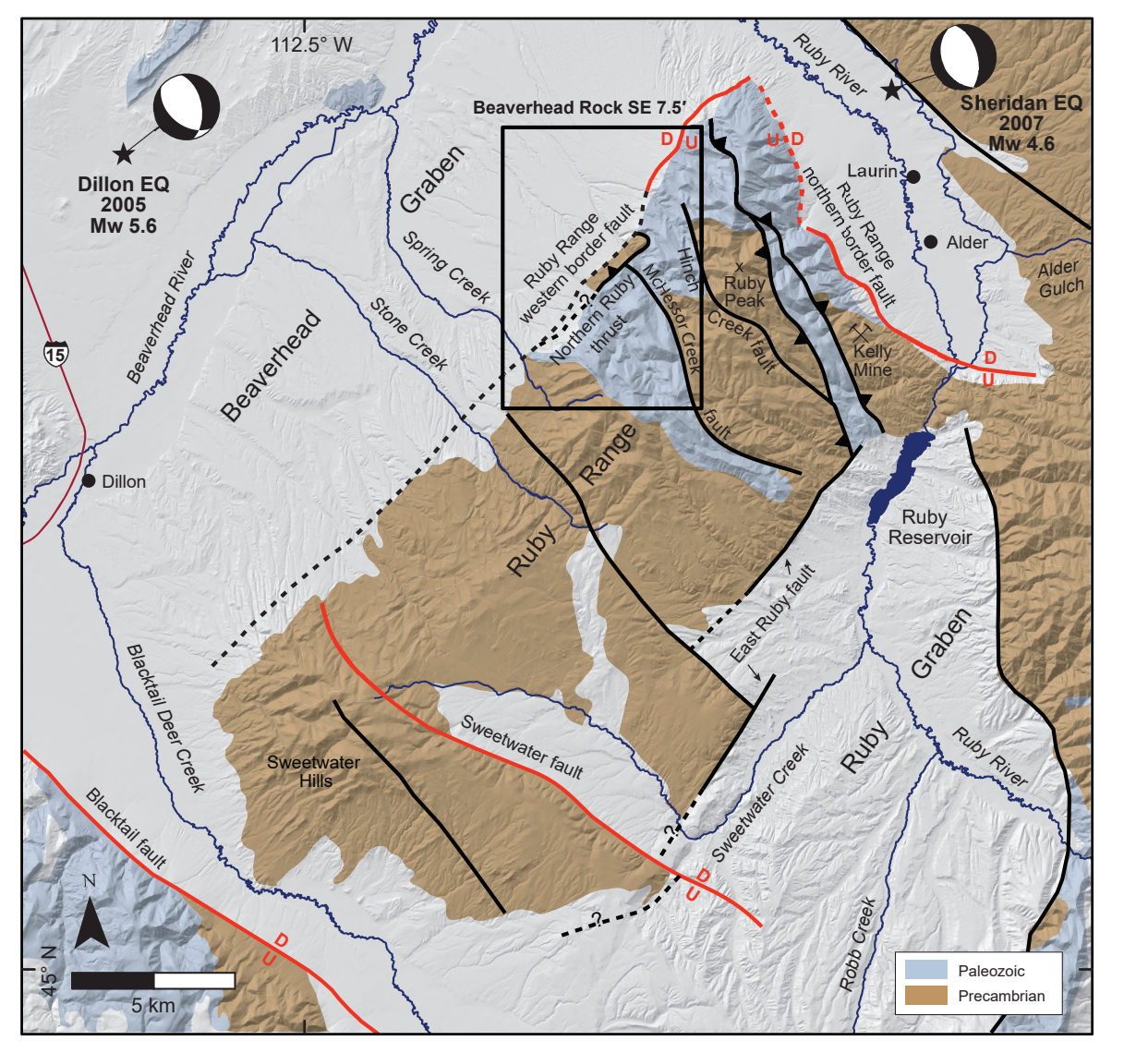

Figure 1. Simplified geologic map of the Ruby Range and surrounding area, showing the general physiography and major faults. Extent of Paleozoic sedimentary rocks and Precambrian crystalline basement rocks modified from Ruppel and others (1993) and Vuke and others (2007). Inset box shows the map area of the Beaverhead Rock SE 7.5′ quadrangle. Faults with Quaternary displacement are shown by red lines. Focal mechanisms shown for recent earthquakes with a magnitude (Mw) > 4.5.

STRUCTURAL GEOLOGY

The northern Ruby Range offers good exposures of the Great Unconformity (see correlation diagram), providing piercing points for documenting multiple fault reactivations since the Precambrian. When the tilt of the overlying Cambrian bedding is restored to horizontal, foliation planes within the Precambrian basement beneath the Great Unconformity dip moderately to the northwest near the Cottonwood Creek fault, but gently to the north near the McHessor Creek fault (fig. 3). This pattern defines a gently north-plunging, miles-long (kilometer scale) anticline in the foliation beneath the Great Unconformity. In both map view and in lower hemisphere stereograms showing poles to planes, the folded geometry of the foliations is similar to bedding of the overlying Paleozoic strata (fig. 4). This correlation may suggest that Precambrian foliations that likely formed during the ca. 1.8–1.7 Ga Big Sky Orogeny, may have also acted as slip surfaces during folding associated with the Cretaceous to Eocene Sevier–Laramide Orogeny (Schmidt and Garihan, 1983). Across the Hinch Creek fault, the Christensen Ranch Metasedimentary Suite appears much thicker in the hanging wall, beneath the Great Unconformity (Parker and Gavillot, 2024). This suggests down-to-the-northeast normal faulting in the Proterozoic, perhaps related to extension in the Belt Basin (Schmidt and Garihan, 1983). Elsewhere in the Ruby Range, Mesoproterozoic dikes show normal offset across fault zones with similar orientations (Wooden and others, 1978).

The Ruby Range is part of the broad northeast-trending basement-cored Blacktail–Snowcrest arch, a regional-scale basement-involved uplift that formed during the Sevier–Laramide Orogeny (e.g., Schmidt and Garihan, 1983). Northeast-dipping basement-involved faults with about 1 mi (2 km) spacing breach southwest-verging anticline–syncline pairs. From west to east, the major basement-involved faults include the Cottonwood Creek, Peterson Creek, McHessor Creek, and Hinch Creek faults (Tysdal, 1981; Schmidt and Garihan, 1983). The systematic northwest plunge of the fault-propagation folds associated with these faults may reflect the gently dipping backlimb of the broad Blacktail–Snowcrest arch (see cross-section; Schmidt and Garihan, 1983). Remnants of foreland basin sediments of the Beaverhead Group (fig. 5) overlie Mississippian and older rocks in the plunging hinges of major synclines. Conglomerates with abundant quartzite clasts (Kbq; figs. 5B–5C) were likely derived from the Belt Supergroup, far to the west. Conglomerates with abundant carbonate and metamorphic clasts (Kbc and Kbcs; figs. 5A and 5D) were locally derived from unroofing of active thrust faults.

The major northeast-dipping thrust faults likely involved some oblique slip (left-lateral), from the total ½–1 mi (1–2 km) of thrust-related throw during regional east–west shortening associated with the Sevier–Laramide Orogeny (see cross-section; Schmidt and Garihan, 1983). The McHessor Creek fault cuts splays of the Peterson Creek fault, consistent with a general west to east progression of deformation. However, the mapped northwest-dipping Northern Ruby thrust (Schmidt and Garihan, 1983) truncates northwest-plunging fault-propagation folds of the other major thrust faults, demonstrating it is a younger, out-of-sequence thrust. Available maximum depositional ages from the Beaverhead Group in the footwall of the Northern Ruby thrust (table 2) suggest that thrusting occurred after ca. 71 Ma. Inversion and reactivation of the Northern Ruby thrust during Cenozoic Basin and Range extension left behind a “perched basement wedge” (Sales, 1983), concealing the basement uplift beneath the Beaverhead Graben.

Northwest-dipping Cenozoic normal faults truncate and deform Precambrian, Mesozoic, and Tertiary units across the northwestern Ruby Range. Fault scarps and deformed alluvial fan deposits suggest Quaternary displacement occurred on the northern section of the Ruby Range western border fault. Vertically offset older alluvial fans (Qafo) and truncated young alluvial fans (Qafy) in the northeast corner of the map suggest that displacement has occurred since the late Quaternary, ca. 130,000 years. ^{26}Al/^{10}Be cosmogenic nuclide burial dating from four cobbles collected within basal gravels in old alluvial fan deposits cut by the fault yielded an isochron age of 2.18 ± 0.08 Ma (table 1; fig. 2; Gavillot and Hidy, in prep.), and further provides *in situ* age control of Quaternary displacement for the Ruby Range western border fault. The Ruby Range western border fault does not exhibit clear fault scarps along the range front in the central and southwest sections of the map. More recent fault displacement could have been accommodated by other unrecognized faults or by blind faulting beneath the Beaverhead Graben, near the epicenter of the 2005 Mw 5.6 Dillon earthquake (fig. 1). The Ruby Range western border fault was mapped as an approximately 24-mi-long (38 km) Quaternary fault by Stickney and others (2000) and is included as a Quaternary fault with poorly constrained timing of faulting within the USGS Quaternary Fault and Fold Database. Fault slip rates are estimated to be less than 0.2 mm/yr, similar to other poorly constrained potential seismogenic faults in southwest Montana (Stickney and others, 2000).

ACKNOWLEDGMENTS

The authors thank John Allard and Katie McDonald, who mapped portions of the quadrangle. We are thankful for the lab assistance from Connie Thompson and Ray Salazar. Thoughtful reviews from Katie McDonald, Michael Stickney, Steven Quane, and Jesse Mosolf helped clarify and improve this report.

DESCRIPTION OF MAP UNITS

Qal **Alluvium (Holocene)**—Unconsolidated, poorly sorted to well-sorted deposits of gravel, sand, silt, and clay deposited by modern streams and creeks. Thickness generally less than 15 ft (5 m) but locally could be up to 30 ft (10 m) within the channel thalweg.

Qaty **Alluvial river terrace (Holocene)**—Unconsolidated, poorly sorted to well-sorted deposits of gravel, sand, silt, and clay deposited as fluvial terraces that stand at slightly higher levels relative to modern channels. Thickness generally less than 15 ft (5 m) above the active channels.

Qafy **Young alluvial fan deposit (Holocene)**—Unconsolidated deposits of clay- to boulder-sized angular to subangular clasts forming incised broad surfaces along the range front and/or near the outlet of major drainages. Deposited as coalescent alluvial fan channels to debris-flow fans. Surfaces of these deposits stand at lower levels than older alluvial fans. Basal contacts of alluvial fans appear to have angular unconformity with underlying Sixmile Creek Formation. Variable thickness, with a maximum of at least 30 ft (10 m) where exposed above its basal contact.

Qct **Calcareous tufa (Holocene to Pleistocene)**—Tan white to light gray calcite-cemented carbonate breccia conglomerate in a porous matrix, and fine-grained calcareous mounds and terraces associated with groundwater and spring deposits. Exposed locally in the hanging wall of the Ruby Range western border fault, north of McHessor Creek. Thickness unknown.

Qac **Alluvium and colluvium (Holocene to Pleistocene)**—Dominantly sand, silt, clay, and subordinate gravel and boulders, deposited on relatively gentle slopes or adjacent to intermountain drainages, primarily by sheetwash and sediment gravity flows. Thickness generally less than 30 ft (10 m).

Qls **Landslide deposit (Holocene to Pleistocene)**—Mass-wasting deposit that consists of unsorted mixtures of clay- to boulder-sized sediment. Color and lithology reflect that of nearby parent rocks and transported surficial material. Variable thickness, typically less than 100 ft (30 m).

Qc **Colluvium (Holocene to Pleistocene)**—Unconsolidated, subangular gravels with local boulders, deposited on hillslopes as debris flows, rock falls, and mass movements. Thickness generally less than 30 ft (10 m).

Qato **Older alluvial river terrace (Pleistocene)**—Unconsolidated, poorly sorted to well-sorted deposits of gravel, sand, silt, and clay deposited as terraces associated with older fluvial to alluvial deposits of northwest-flowing drainages of the western Ruby Range. Surfaces of these deposits stand at higher levels than younger terrace deposits and modern channels. Thickness generally less than about 30 ft (10 m).

Qafo **Older alluvial fan deposit (Pleistocene)**—Unconsolidated deposits of clay- to boulder-sized subangular to angular clasts forming deeply incised broad surfaces along the range front and/or near the outlet of major drainages. Deposited as coalescent alluvial fan channels and debris flow fans. Surfaces of these deposits stand at higher levels than younger alluvial fans. Basal contacts of alluvial fans have an angular unconformity with underlying Sixmile Creek Formation. Variable thickness, with a maximum of at least 30 ft (10 m). ^{26}Al/^{10}Be cosmogenic nuclide burial dating from four cobble samples collected within the unit basal gravels yielded an isochron age of 2.18 ± 0.08 Ma (table 1; figure 2; Gavillot and Hidy, in prep.).

Tsc **Sixmile Creek Formation (Miocene)**—Unconsolidated conglomerate deposits of cobble- to boulder-sized subangular to angular clasts and a matrix of medium- to coarse-grained sandstone. Underlies Quaternary alluvial fan deposits and surfaces. Likely deposited as older sequences of alluvial fan deposits that show tilted gravel beds of 7–10° compared to sub-horizontal Quaternary deposits. U-Pb zircon dates from a sandstone sample near the Ruby Range western border fault, south of Trout Creek, yield a maximum depositional age of 7.3 ± 0.1 Ma (table 2; fig. 6A; Brennan and others, in prep.), supporting a correlation with the Sixmile Creek Formation. Total thickness unknown but is at least 70 ft (20 m) thick.

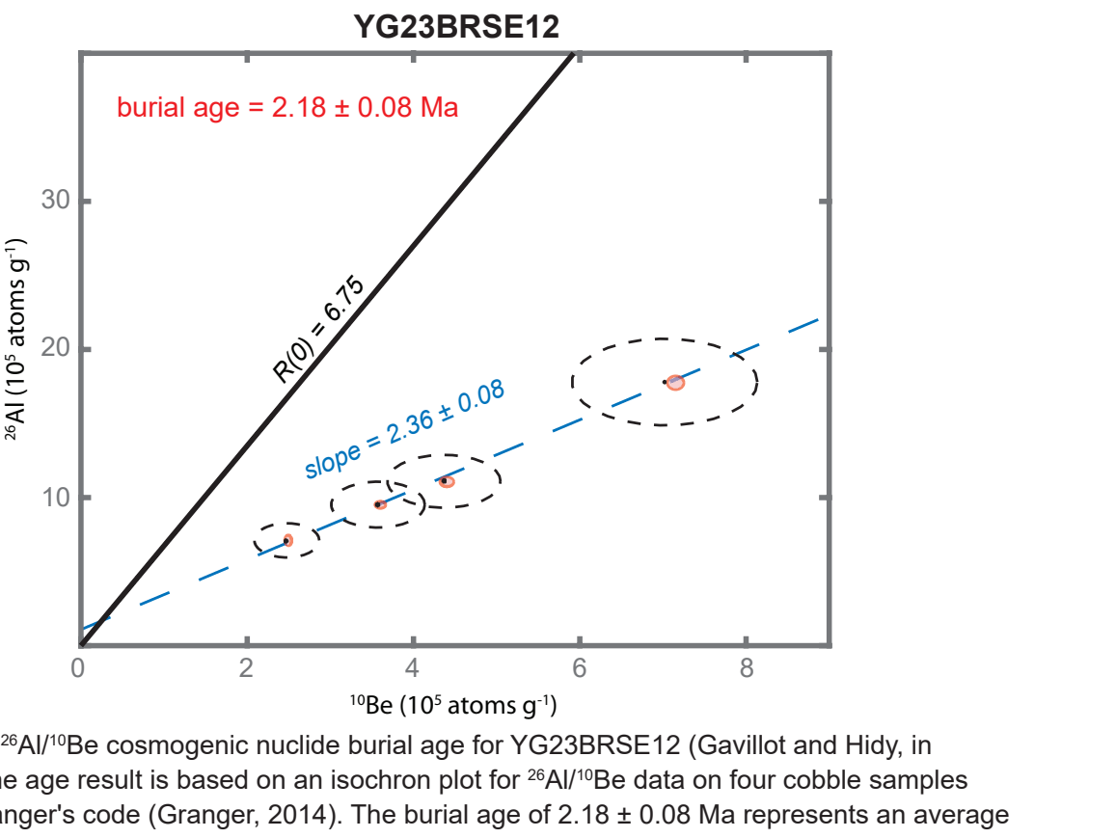

Figure 2. ^{26}Al/^{10}Be cosmogenic nuclide burial age for YG23BRSE12 (Gavillot and Hidy, in prep.). The age result is based on an isochron plot for ^{26}Al/^{10}Be data on four cobble samples using Granger's code (Granger, 2014). The burial age of 2.18 ± 0.08 Ma represents an average of five individual model age runs. Model inputs for these gravels buried 26 ft (8 m) below the ground surface are based on the watershed source parameters of these cobbles within McHessor Creek in the Ruby Range. Watershed source average elevation: 7,382 ± 1,345 ft (2,250 ± 410 m). Watershed source average latitude: 45.2981.

Table 1. ^{26}Al/^{10}Be sample data and burial age for YG23BRSE12.

Sample[a]	Clast Lithology[b]	Quartz mass (g)	^{26}Al/^{27}Al (x10^{-15})		^{26}Al concentration		^{10}Be/^{9}Be (x10^{-15})		^{10}Be concentration		^{26}Al/^{10}Be		Age (Ma)[d]
			Ratio	(±1σ)	(10^3 atoms/g qtz)	(±1σ)	Ratio	(±1σ)[c]	(10^3 atoms/g qtz)[c]	(±1σ)[c]	Ratio	(±1σ)[c]	
McHessor Creek buried gravels													
YG23BRSE12-QTg7	quartzite	25.03	260.62	10.4180	1105.3220	45.6553	865.7525	16.5762	440.0752	8.4612	2.51	0.11	2.18 ± 0.08
YG23BRSE12-QTg8	quartzite	19.99	247.70	11.5016	712.8048	33.9997	390.4548	7.2572	249.7349	4.6737	2.85	0.15	
YG23BRSE12-QTg10	gneiss	30.00	503.83	15.6348	951.5098	30.4316	838.8850	15.4670	360.2712	6.6700	2.64	0.1	
YG23BRSE12-QTg13	gneiss	25.37	435.46	9.9505	1775.1150	42.9805	1406.6563	19.6163	715.2769	10.0308	2.48	0.07	

[a] Samples represent a suite of cobble-size clasts from the same stratigraphic interval of buried gravels with an average sampling depth of 26 ft (8 m) below the modern ground surface of younger alluvial fan deposits (Qafy). Buried gravels location: Lat = 45.3655; Long = -112.3393; Elevation = 5,430 ft (1,655 m).

[b] Sampled lithologies (quartzite and gneiss) reflect various clast sources mapped within the McHessor Creek watershed that include the Beaverhead Group, Flathead Formation, Christensen Ranch Metasedimentary Suite, and Dillon gneiss.

[c] All uncertainties reported at 1σ. Blank corrected for ^{26}Al/^{27}Al and ^{10}Be/^{9}Be ratios. Total measurement uncertainty for the ^{26}Al and ^{10}Be concentrations includes the uncertainty in the ^{27}Al and ^{9}Be carrier concentrations, AMS measurement uncertainty, and uncertainty in the process blank correction. Combined, these uncertainties totaled to within 1σ.

[d] Cosmogenic nuclide burial age report using ^{26}Al/^{10}Be from Gavillot and Hidy (in prep.). The age result is based on an isochron plot for ^{26}Al/^{10}Be data on four YG23BRSE12 cobble samples using Granger's linearization code and isochron script (Granger, 2014).

Kbcs **Conglomerate and sandstone of the Beaverhead Group (Late Cretaceous)**—Indurated interbedded conglomerate gravels in a light brown sand matrix and pebble to fine-grained sandstone with trough cross-bedding and grading, subrounded to subangular pebble- to cobble-sized clasts derived primarily from basement gneiss, and subordinate Paleozoic carbonates (fig. 5D). Locally olive to dark gray mudstone and siltstone. Unit exposed along the western Ruby Range front. Previously mapped as part of the Lower Bozeman Group (Oligocene–Lower Eocene) by Tysdal (1976). However, U-Pb zircon dates from a sandstone in the footwall of the Northern Ruby thrust, north of McHessor Creek, yield a maximum depositional age of 71.0 ± 0.5 Ma (table 2; fig. 6B; Brennan and others, in prep.), suggesting that the unit is age correlative with the quartzite conglomerate of the Beaverhead Group (Kbq). Total thickness unknown, at least 500 ft (150 m).

Kbq **Quartzite conglomerate of the Beaverhead Group (Late Cretaceous)**—Indurated conglomerate gravels in dark brownish red sand matrix and local coarse sandstone beds with well-rounded fluvial pebbles to boulder-sized quartzite clasts, likely derived from Belt Supergroup rocks. Good exposures occur north of McHessor Creek as steeply dipping resistant outcrops (fig. 5B). In other places, unit consists of unconsolidated, well-rounded fluvial cobbles to boulders derived from quartzite and subordinate Paleozoic carbonates, basement gneiss, and Cretaceous volcanic dacite cobbles (fig. 5C). Unconsolidated conglomerate near Spring Canyon lacks carbonate and basement clasts and can be traced into the footwall of the Spring Canyon thrust, supporting correlation with the quartzite conglomerate of the Beaverhead Group in the neighboring Laurin Canyon 7.5′ quadrangle (Parker and Gavillot, 2024). Unit exposed along the western Ruby Range front. Unconformable basal contact with folded Mississippian carbonates. In numerous places the upper conglomerate stratigraphy is juxtaposed to a thrust fault. U-Pb zircon dates from a sandstone lens in the footwall of the Northern Ruby thrust, north of McHessor Creek, yield a maximum depositional age of 74.9 ± 0.5 Ma (table 2; fig. 6C; Brennan and others, in prep.). U-Pb zircon dating of dacite cobbles within the unit yielded similar maximum depositional ages of ca. 71–75 Ma (table 2; Mosolf and others, 2023a). Total thickness unknown, at least 400 ft (120 m).

Kbc **Carbonate conglomerate of the Beaverhead Group (Late Cretaceous)**— Indurated conglomerate gravels in a reddish orange sand matrix cemented with calcium carbonate and subangular to rounded pebble- to boulder-sized clasts derived primarily from the Mississippian carbonates with subordinate clasts of basement gneiss and other Paleozoic carbonates (fig. 5A). Locally with thin layers of mudstone. Unit exposed along the western range front of the Ruby Range. Good exposures occur just north of McHessor Creek. In the Bannack 7.5′ quadrangle near Dillon (fig. 1), a similar conglomerate is overlain by the Cold Spring Creek Volcanic Group (Late Cretaceous) emplaced ca. 72–73 Ma (table 2; Mosolf, in review). In the Beaverhead Rock SE map area, a dated Cretaceous dacite lava flow yielded an age of 72.3 ± 0.8 Ma (Mosolf and others, 2023a), and may similarly provide an upper age constraint of this carbonate conglomerate. Total thickness unknown, at least 400 ft (120 m).

Kda **Dacite (Late Cretaceous)**—Black, brown-red weathering porphyritic to vesicular dacite lava flow (67.4 wt. percent SiO^2, fig. 6, Mosolf and others, 2023b) and dacitic tuff. Fine-grained pyroxene and plagioclase phenocrysts are common. Phenocrysts are often weathered out, leaving behind angular voids. Rests unconformably on folded Mississippian carbonates. U-Pb zircon dating yielded a weighted mean age of 72.3 ± 0.8 Ma, with inherited Mesoproterozoic to Archean grains (table 2; Mosolf and others, 2023a). Thickness unknown.

Mlb **Lombard Formation of the Snowcrest Range Group (Mississippian)**—Light brown to gray, lavender-weathering micrite with ½-ft-scale (dm-scale) to ½-in-scale (cm-scale) tabular bedding. Irregularly shaped orange to tan grainy nodules may reflect partial chert growth. Rarely exposed, except in the footwall of the Hinch Creek fault in the northeastern part of the map. Upper contact is not constrained in the quadrangle. Conodonts and available marine fossils suggest a late Mississippian age (Meramecian to Chesterian; Sando and Sandberg, 1985; Wardlaw and Pecora, 1985). Thickness is at least 220 ft (67 m), based on a section measured in the northern Ruby Range (Tysdal, 1970).

Mk **Kibbey Formation of the Snowcrest Range Group (Mississippian)**—Maroon to light gray, red-weathering, fine-grained muddy quartz arenite and interbedded lavender micrite with platy ½-in-scale (cm-scale) bedding. Crude, low-relief channels and crossbeds are common. Commonly forms red slopes in the footwall of the Hinch Creek fault in the northeastern part of the map. Conodont fossils suggest a late Mississippian (Meramecian) age (Sando and Sandberg, 1985). At least 140 ft (43 m) thick based on measured section in the northeastern part of map (Tysdal, 1970).

Mmc **Mission Canyon Formation of the Madison Group (Mississippian)**—Light gray weathering, massive cliff-forming limestone. Sparry cement often obscures primary crinoidal packestone lithology. Commonly brecciated. Upper part resembles the Lodgepole Formation, with tabular sparry limestone beds and bedded nodular chert. Basal contact placed at the lowest cliff of massive limestone. Upper contact is an unconformity marked by a sharp color change from gray to bright red. Conodont fossils suggest a late Mississippian (Osagean to Meramecian) age (Sando and Sandberg, 1985). Thickness is about 920 ft (280 m) in the northeastern part of map (Tysdal, 1970).

MDlst **Lodgepole (Madison Group), Sappington, and Three Forks Formations, undivided (Mississippian to Devonian)—**

Lodgepole Formation—Gray to lavender tabular bedded micrite and wackestone, with yellow silty partings, grades downward into laminated gray to lavender micrite with thin continuous to stringy discontinuous orange-brown weathering chert beds. Tabular bedding dominates, on the ½-in-scale (cm-scale) to ½-ft-scale (dm-scale), particularly in the upper part. Upper part contains highly fossiliferous wackestone beds with sharp scoured bases that fine up into micrite, with silty parting containing abundant bed parallel trace fossils and *Zoopyhcos*. Intact crinoids, fenestrate bryozoans, bivalves, and disarticulate brachiopods including *Orthotetes* fossils are common, especially near the uppermost part. Mostly covered by talus slopes, with platy to chippy float characterizing the lower part. Upper contact is placed below the first massive cliff-forming limestone of the Mission Canyon Formation. Internal contact between Lodgepole and Sappington Formations is mapped where contact is confidently placed, at the lowest laminated micrite bed. Early to Middle Mississippian (Kinderhookian to Osagean) in age (Sando and Dutro, 1974). Thickness about 700 ft (213 m).

Sappington Formation—Yellow-weathering partly calcareous siltstone to very fine-grained sandstone. Not exposed in the quadrangle. In the neighboring Laurin Canyon 7.5′ quadrangle (Parker and Gavillot, 2024), the measured thickness is 70 ft (21 m; di Pasquo and others, 2017). Latest Devonian (late Famennian) in age (di Pasquo and others, 2017).

Three Forks Formation—Light mint green to deep red chippy mudstone, siltstone, and breccia and light gray-brown, orange-weathering micrite with mud chip breccia. Rarely exposed. These lithologies likely belong to the Logan Gulch Member, in the lower part of the unit. The upper part of the unit (Trident Member) is rarely exposed. Uncommon silty limestone exposures may belong to either the Knoll limestone at the top of the Logan Gulch Member or the Trident Member (Sandberg, 1965). Latest Devonian (early to middle Famennian) in age (di Pasquo and others, 2017). Thickness is poorly constrained, but is likely around 80 ft (25 m).

Dj **Jefferson Formation (Devonian)**—Gray to bleached white tabular bedded crystalline dolostone, and uncommon brown brecciated dolostone beds. Recessive with sparse outcrops, often with “elephant skin” weathering. Pervasive secondary dolomite obscures much of the original sedimentary structure, although mottled textures remain common. Rare cycles of laminated to thick-bedded tabular mottled dolostone, as well as graded bedding, mud chips, and flat laminations. A marker cliff-forming, tabular vitreous white dolostone bed [3–6 ft (1–2 m)] occurs near the base of the formation in many places. Lower contact is placed below the lowest pure dolostone bed, above siliciclastic and grainy-weathering dolostone intervals. Upper contact is placed below the lowest slope of chippy limestone or siltstone float. Likely Late Devonian in age (e.g., Dorobek and others, 1991). A thickness of 268 ft (82 m) was measured in McHessor Creek (Tysdal, 1970).

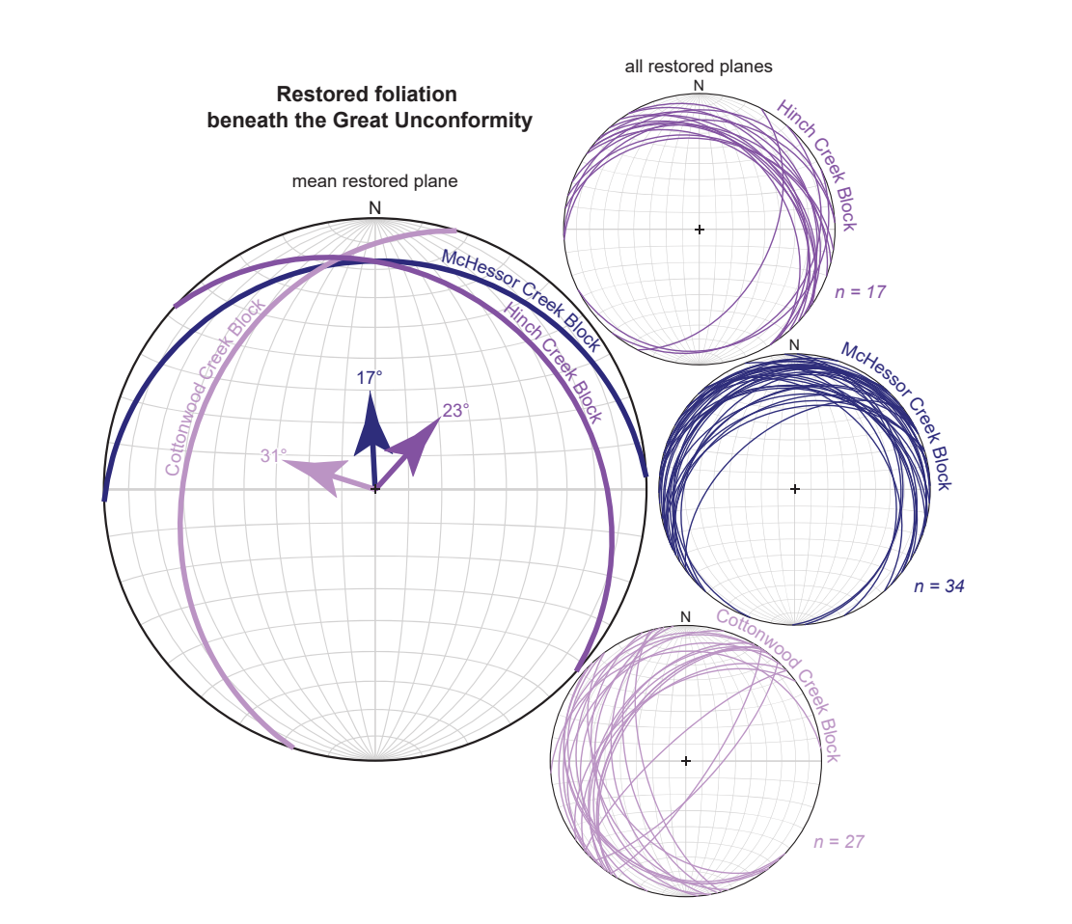

Figure 3. Lower hemisphere stereographic projection of restored metamorphic foliation planes immediately beneath the Great Unconformity, from the map area in the Beaverhead Rock SE quadrangle and neighboring Laurin Canyon 7.5′ quadrangle (Parker and Gavillot, 2024). Metamorphic foliation planes were rotated along with measured bedding planes immediately above the Great Unconformity until bedding was schematically restored to horizontal. Mean restored planes shown in large stereogram, with arrows showing dip direction and magnitude. Small stereograms show all restored planes for each respective structural block. The hanging wall of the particular fault defines the structural block.

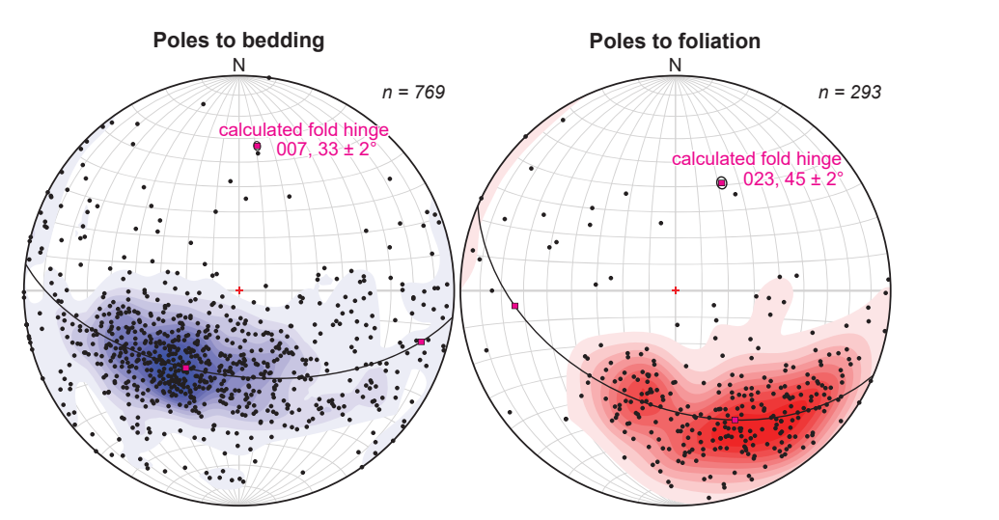

Figure 4. Lower hemisphere stereographic projections of poles to bedding for folded Paleozoic rocks (left) and poles to metamorphic foliation for folded Precambrian rocks (right). Shading denotes Kamb contouring at 2σ uncertainty envelopes. Calculated best-fit girdle and fold hinge are shown, with 2σ uncertainty labeled.

Ꞓrpi **Red Lion and Pilgrim Formations, undivided (upper Cambrian)**—Tan, tabular to massive, grainy-weathering dolostone, gray to tan wavy thin-tabular bedded (“ribboned,” Tysdal, 1970) dolo-wackestones with pale green to red silty partings and uncommon cross-bedded quartz arenite with dolomite cement. Laminated and mottled beds are common. Recrystallized dolomite mudchips are uncommon. Lower portion forms prominent cliffs and is carbonate rich, while upper portion contains more siliciclastic material, including ribbon rock. Cross-bedded sandstone is a persistent marker bed, near the upper part of the Pilgrim Formation. “Ribboned” rock assigned to the Red Lion Formation (Tysdal, 1970) occurs both above and below the cross-bedded sandstone marker bed of the Pilgrim Formation. Ribbon rock varies from graded dolostone beds with trace amounts of siliciclastics to red, graded, very fine-grained sandstone to siltstones with rippled muddy partings and extensive bioturbation. Gradational contacts separate these lithologies at multiple stratigraphic positions, and along-strike changes in thickness and lithology are common. A 2 ft (<1 m) green shale interval is rarely observed, in sharp contact above the Pilgrim Formation and below ribbon rock. This shale was interpreted by Tysdal (1970) as a sequence boundary, marking the base of the Dry Creek Member of the Red Lion Formation. The Red Lion Formation may largely be absent in the quadrangle, except where the internal contact of the shale interval has been mapped. Lower contact is marked by the lowest outcrop of dolostone. Upper contact is placed below the first resistant thick-bedded bleached crystallized dolomite bed of the Jefferson Formation. Age is likely upper Cambrian based on correlative strata in southwestern Montana (e.g., Bush and others, 2012; Link and others, 2017). A thickness of 560 ft (170 m) was measured in McHessor Creek (Tysdal, 1970).

Ꞓp **Park Formation (middle Cambrian)**—Green shale and rare brown to tan limestone pebble conglomerate. Rarely crops out, and more commonly forms soft, recessive slopes of green to maroon shale with gray-lavender to orange micrite, and rare red oncoid limestone float. Common detachment surface for landslides. Fossils collected in the quadrangle suggest a middle Cambrian age (Tysdal, 1970). A thickness of 175 ft (53 m) was measured in McHessor Creek (Tysdal, 1970).

Ꞓm **Meagher Formation (middle Cambrian)**—Mottled red to tan weathering sparry dolomite in gray fine-grained limestone micrite, and heavily recrystallized dolo-packestones and ooid grainstones. Characteristic mottled lime–dolostone intervals are more common in lower half. Micrite laminations, ooids, pisoids, and mudchips common but difficult to see due to grainy dolomite recrystallization of mud. Heavily bioturbated in most beds. Branching ½-in-scale (cm-scale) burrows (twiggy forms of Tysdal, 1970) are uncommon. Bedding is typically thin, wavy tabular, to 1-ft-scale (⅓-m-scale) planar tabular with pronounced light and dark gray mottling. Lower part often forms talus slopes, with upper part forming prominent cliff bands. Fossils collected in the quadrangle suggest a middle Cambrian age (Tysdal, 1970). At least 745 ft (227 m) thick, based on a measured section in McHessor Creek (Tysdal, 1970).

Ꞓwf **Wolsey and Flathead Formation, undivided (middle Cambrian)—**

Wolsey Formation—Green, papery, micaceous shale. Rarely outcrops, and more often forms swales with rare green chippy shale float. Variable thickness, with 47 ft (14 m) measured in the neighboring Laurin Canyon 7.5′ quadrangle (Tysdal, 1970).

Flathead Formation—Tan, orange- to red-weathering medium-grained quartz arenite. Ranges from fine to very coarse, sometimes micaceous or glauconitic, moderately to well-sorted with subrounded to well-rounded, sometimes frosted grains. Bedding is typically tabular to massive or trough cross-bedded, with rare foot-scale (meter-scale) foresets and ripples. Rare vertical burrows. Lower contact is the angular Great Unconformity. Age of both units is likely middle Cambrian (e.g., Thomas, 2007; Bush and others, 2012). Upper contact placed at base of talus slope of lower Meagher Formation. Variable thickness, with 58 ft (18 m) measured in the neighboring Laurin Canyon 7.5′ quadrangle (Tysdal, 1970).

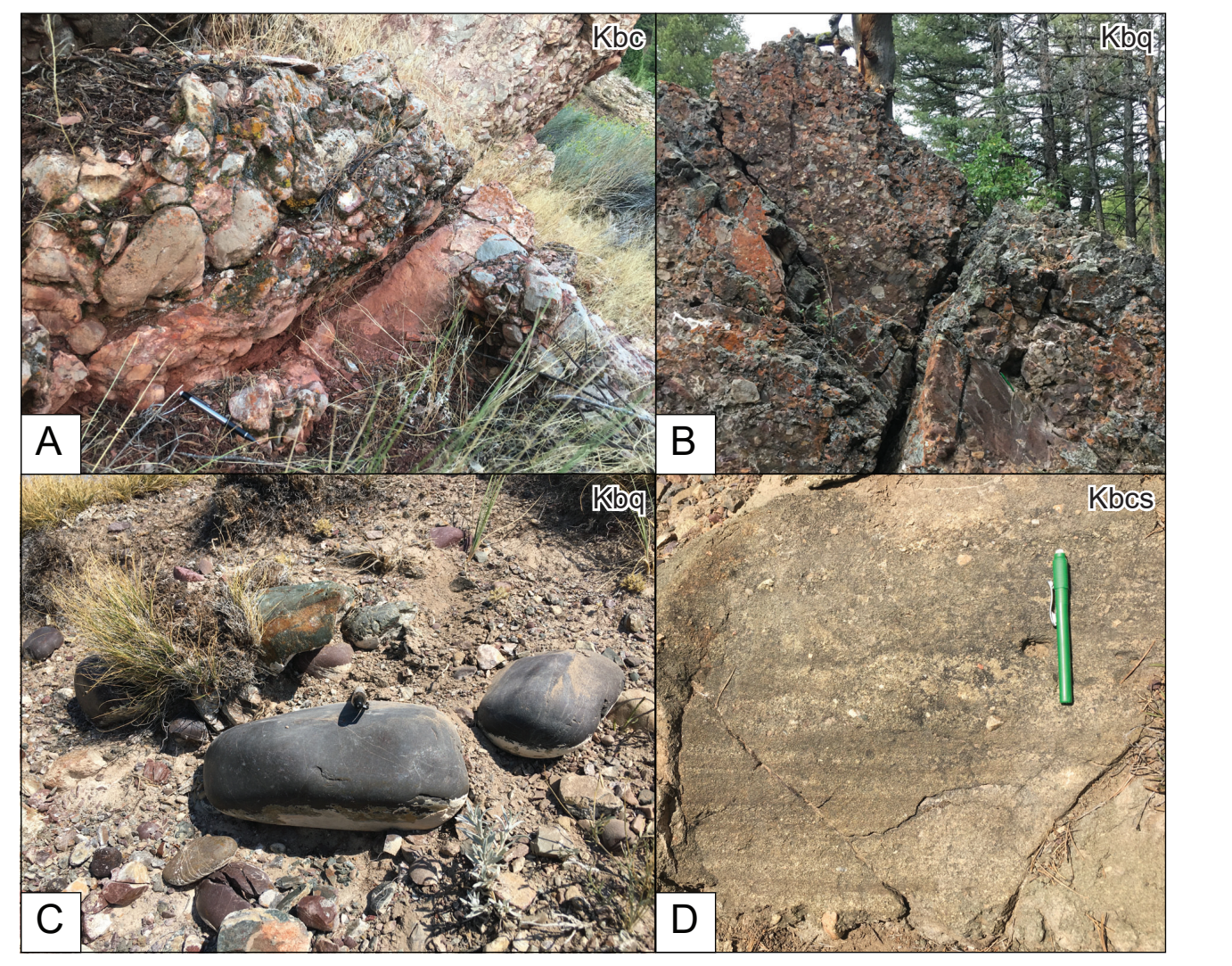

Figure 5. Field photographs of Cretaceous conglomerates from locations north of McHessor Creek. (A) Well-exposed outcrops of 44°NE-dipping carbonate conglomerate member of the Beaverhead Group (Late Cretaceous; Kbc) with a thin red mudstone bed. (B) Well-exposed outcrops of 40°NE-dipping quartzite conglomerate member of the Beaverhead Group (Late Cretaceous; Kbq) with a medium to thick-bedded red sandstone. (C) Poorly exposed outcrops of quartzite conglomerate member of the Beaverhead Group (Late Cretaceous; Kbq), with abundant quartzite cobbles and pervasive fracturing of clasts. (D) View looking straight down of well-exposed outcrops of overturned to steeply dipping conglomerate and cross-bedded sandstone sourced primarily from basement gneiss (Kbcs).

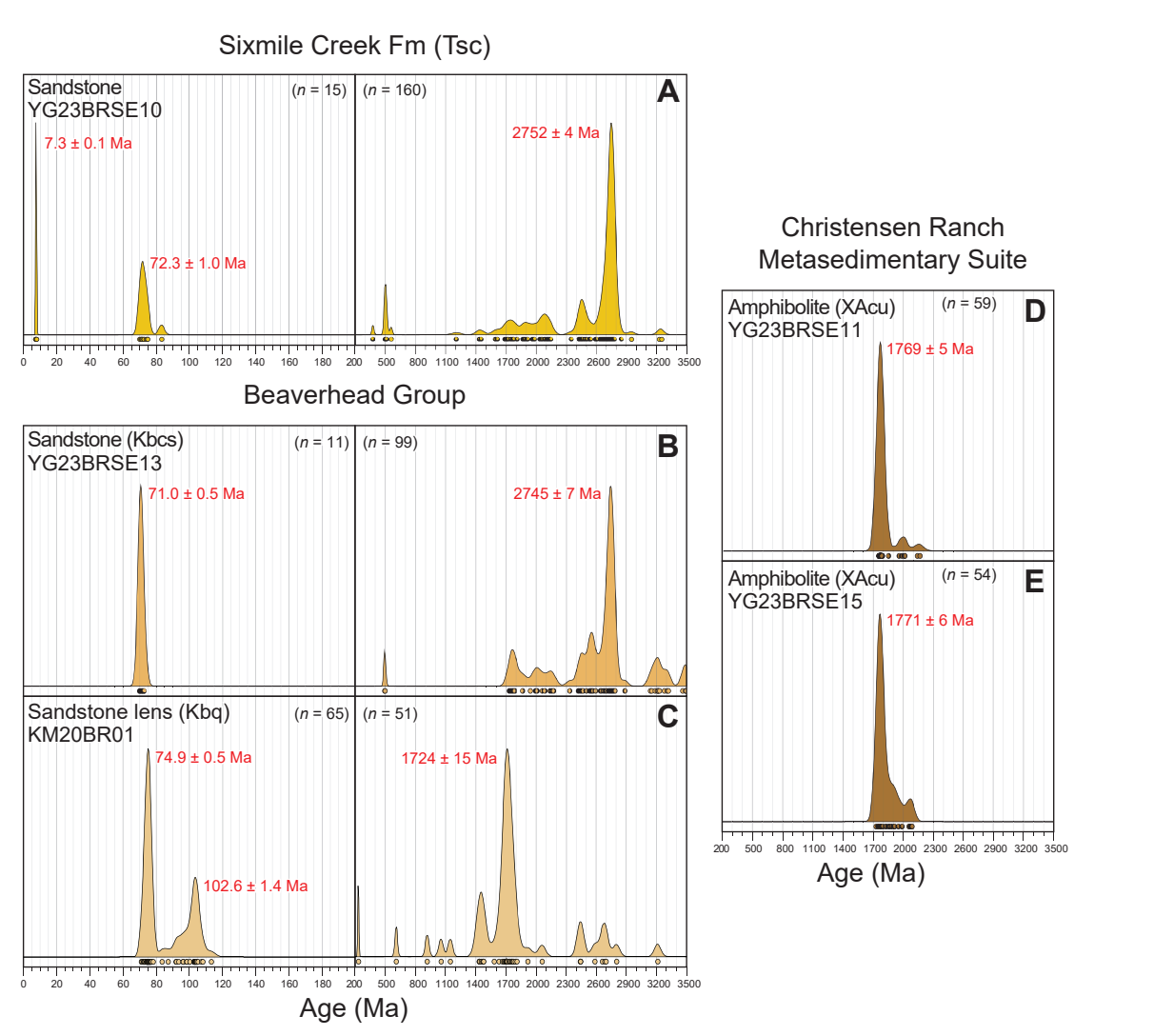

Figure 6. Probability density plots (PDPs) of ^{207}Pb corrected ^{206}Pb/^{238}U (<1,400 Ma) and ^{207}Pb/^{206}Pb (>1,400 Ma) zircon ages with less than 10% discordance for samples in the Sixmile Creek Formation (A), Beaverhead Group (B–C), and Christensen Ranch Metasedimentary Suite (D–E). Bandwidths and bin widths of 5 m.y. were used for KDE plots between 0 and 200 Ma and 10 m.y. and 50 m.y., respectively, for KDE plots between 200 and 3,500 Ma. Circles show individual age analyses. See table 2 for more information regarding weighted mean ages. Data reported in Mosolf and others (2023a), and Brennan and others (in prep.).

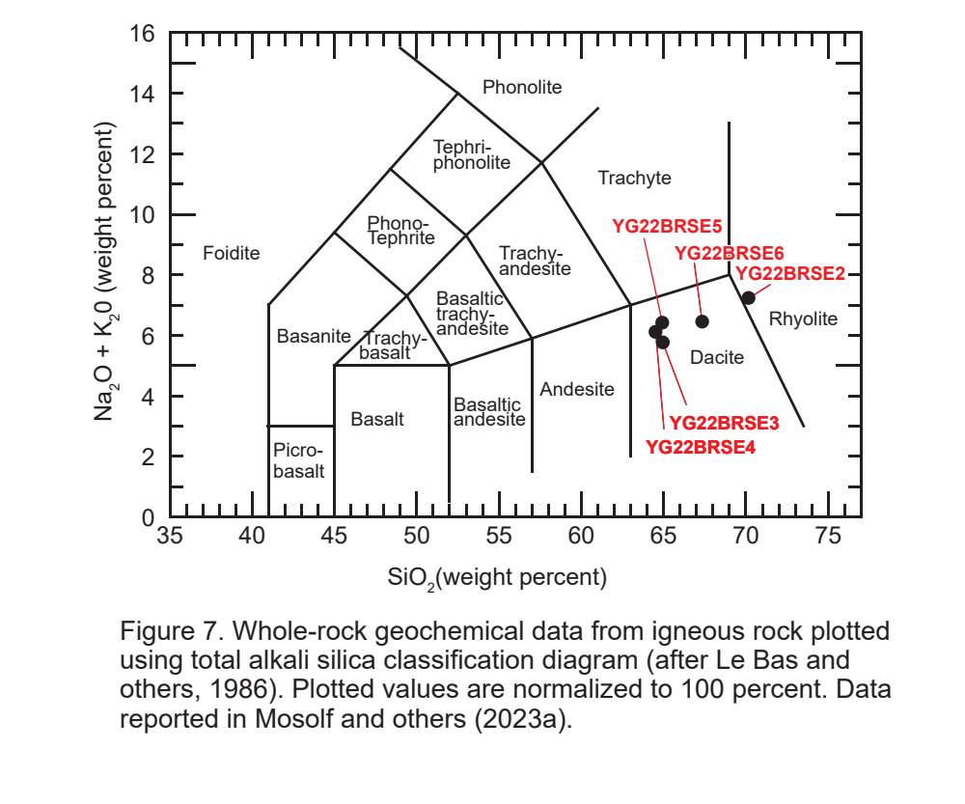

Figure 7. Whole-rock geochemical data from igneous rock plotted using total alkali silica classification diagram (after Le Bas and others, 1986). Plotted values are normalized to 100 percent. Data reported in Mosolf and others (2023a).

Table 2. U-Pb zircon geochronology.

Sample	Lithology	Unit	Latitude (°N)	Longitude (°W)	No. of Spot Analyses[a]	Weighted Mean Age (Ma)	2σ	MSWD
YG23BRSE10	sandstone	Tsc	45.2930	-112.3377	2/175	7.3	0.1	0.5
YG23BRSE13	sandstone	Kbcs	45.3167	-112.2875	11/111	71.0	0.5	1.1
YG22BRSE2	dacite cobble in gravel	Kbq	45.3590	-112.2661	39/40	73.0	0.6	1.5
YG22BRSE3	dacite cobble in gravel	Kbq	45.3603	-112.2710	35*/40	74.1	0.3	0.5
YG22BRSE4	dacite cobble in gravel	Kbq	45.3605	-112.2712	36*/40	75.2	0.3	1.4
YG22BRSE5	dacite cobble in gravel	Kbq	45.3639	-112.2641	27/72	71.3	0.6	2.0
KM20BR01	sandstone	Kbq	45.3245	-112.2827	36*/116	74.9	0.5	2.9
YG22BRSE6	dacite lava flow	Kda	45.3429	-112.2687	6/67	72.3	0.8	1.9
YG23BRSE11	amphibolite	XAcu	45.2929	-112.3352	52/59	1769.4	5.2	0.2
YG23BRSE15	amphibolite	XAcu	45.3251	-112.2926	38/54	1771.4	6.0	0.3

Note. Reported ages are the weighted mean of the ^{207}Pb corrected ^{206}Pb/^{238}U ages for dates <1,400 Ma, and ^{206}Pb/^{238}U ages for dates >1,400 Ma. Only dates with <10% discordance were used in age calculations. MSWD is the Mean Square Weighted Deviation. Reported 2σ uncertainties take into account overdispersion. Zircon separates were prepared at MBMG and analyzed by LA-ICP-MS at the University of California, Santa Barbara. Latitudes and longitudes are in the 1984 World Geodetic Survey (WGS84) datum.

[a] Numerator denotes the number of spot analyses used to calculated weighted mean age; denominator denotes the total number of concordant analyses in the sample.

*Weighted mean calculations allowed for rejection of outliers via a modified 2σ set of criteria (Ludwig, 2012), and the number of accepted analyses included in the weighted mean calculations is reported.

Christensen Ranch Metasedimentary Suite (CRMS)

XAcu ***Undifferentiated metasedimentary rocks and gneiss (Paleoproterozoic to Archean?)***— A variety of metasedimentary rocks, including: marble, quartz–biotite–garnet and rare phlogopite–sillimanite–garnet schist, and vitreous white to green micaceous quartzite and schist with uncommon biotite and garnet. Plagioclase–horneblende–diopside gneiss with uncommon biotite and garnet is a marker unit near the Kelly Mine area in the neighboring Laurin Canyon 7.5′ quadrangle (James, 1990). While these lithologies are distinctive for the CRMS, the most abundant lithologies are intermediate to felsic quartzofeldspathic gneiss with uncommon garnet and amphibolite. While a thick marble unit reliably marks the base of the suite in neighboring studies (James, 1990; Jones, 2008), it is typically bounded on both sides by quartzofeldspathic gneiss and amphibolite, making it difficult to differentiate the Christensen Ranch Suite from the Dillon Gneiss without more complete exposures of the metasedimentary lithologies not available in the map area. U-Pb dating of monazite within schist, amphibolite, and gneiss yielded ages ranging from ca. 1.75 to 1.81 Ga constraining peak metamorphism (Jones, 2008; Cramer, 2015). U-Pb dating of zircon from two samples of amphibolite within the map area reveals a similar age population of ca. 1.77 Ga (figs. 6D, 6E, Brennan and others, in prep.). Apparent structural thickness up to about 5,000 ft (1,500 m) in the southern part of the map.

XAcm ***Marble (Paleoproterozoic to Archean?)***—White to gray, tan to brown-weathering medium to coarsely crystalline dolomitic and calcitic marble with local boudins of quartzite. Ranges from massive to weakly foliated, moderately resistant outcrop bands. Magnetite and diopside are the predominant accessory minerals. Phlogopite and tremolite in impure layers are not common. Dolomitic beds tend to be thicker, cleaner, and more monomineralic, while calcitic beds seem to be thinner, more isolated, and with more calc–silicate minerals. Talc is also locally common in coarse dolomite marble, near Ruby Peak (Tysdal and others, 1987). Apparent thickness of up to about 1,800 ft (550 m) in the southern part of the map.

XAam **Amphibolite (Paleoproterozoic to Archean)**—Foliated to massive, medium- to coarse-grained black and white, brownish-weathering horneblende–plagioclase ± garnet amphibolite. Nearly equal parts amphibole and plagioclase give it a characteristic “salt and pepper” appearance. Coarse quartz stringers are common. Epidote, actinolite, diopside, and chlorite are not common. Forms resistant outcrops in lenses, pods, and boudins. Commonly interlayered with all other Archean to Paleoproterozoic lithologies, but only mapped in the thick package exposed in the upper reaches of McHessor Creek, in the eastern part of the map. Whole-rock geochemistry is similar to tholeiitic basalt composition, suggesting a mafic igneous rock protolith (Wilson, 1981; James, 1990; Mosolf and others, 2023b). Apparent thickness of about 1,050 ft (320 m).

Adg **Dillon Gneiss (Archean)**—Foliated, gray-white to pink, reddish brown-weathering, felsic to intermediate microcline–quartz–plagioclase ± biotite ± garnet ± hornblende gneiss and migmatite with interlayered black, coarse- to medium-grained amphibolite. Minor granite (quartz–microcline) pegmatite dikes, intrusions, and gneisses and quartz–plagioclase ± garnet leucogneiss. Leucogneiss is often mylonitized, with quartz and feldspar ribbons defining a lineation and foliation. Generally recessive, forming sparsely vegetated slopes. The wide range of lithologic variation observed on the outcrop scale may represent a complex sedimentary, volcanic, and igneous protolith (James and Hedge, 1980; James, 1990). In the southwestern Ruby Range, average composition of the Dillon Gneiss is granitic, with a mean of 74 weight percent SiO$_2$ (James, 1990), with 42 percent microcline, 31 percent quartz, and 27 percent plagioclase (Garihan and Williams, 1976). South of the quadrangle, U-Pb dating of zircon reveals age populations of ca. 2.77, 2.47, and 1.78 Ga (Jones, 2008; Stotter, 2019). A mylonitic garnet leucogneiss has been dated to 2.5 Ga, constraining the protolith age to Archean (Harms and Baldwin, 2023). Apparent thickness of at least about 3,800 ft (1,150 m).

REFERENCES

Brennan, D., Parker, S.D., Mosolf, J.G., and Kylander-Clark, A., in preparation, U-Pb geochronology data from rock samples collected in the Dillon, Polson, and Wisdom 30′ x 60′ quadrangles, western Montana, 2022–2023: Montana Bureau of Mines and Geology Analytical Dataset.

Bush, J.H., Thomas, R.C., and Pope, M.C., 2012, Sauk megasequence deposition in northeastern Washington, northern Idaho, and western Montana, *in* Derby, J.R., Fritz, R.D., Longacre, S.A., Morgan, W.A., and Sternbach, C.A., eds., The great American carbonate bank: The geology and economic resources of the Cambrian-Ordovician Sauk megasequence of Laurentia: American Association of Petroleum Geologists Memoir, v. 98, p. 751–768.

Cramer, M., 2015, Proterozoic tectonometamorphic evolution of the Ruby Range, SW Montana, USA: Insights from phase equilibria modeling and *in situ* monazite petrochonology: Missoula, University of Montana, M.S. thesis, 120 p., scale 1:24,000.

di Pasquo, M., Grader, G.W., Warren, A., Rice, B., Isaacson, P., and Doughty, P.T., 2017, Palynologic delineation of the Devonian-Carboniferous boundary, west-central Montana, USA: Palynology, v. 41, no. S1, p. 189–220.

Dorobek, S.L., Reid, S.K., Elrick, M., Bond, G.C., and Kominz, M.A., 1991, Subsidence across the Antler foreland of Montana and Idaho: Tectonic versus eustatic effects: Kansas Geological Survey Bulletin, v. 233, p. 232–251.

Garihan, J.M., and Williams, K., 1976, Petrography, modal analyses and origin of Dillon quartzo-feldspathic and pre-Cherry Creek gneisses, Ruby Range, southwestern Montana: Northwest Geology, v. 5, p. 42–49.

Gavillot, Y., and Hidy, J., Alan, in preparation, Cosmogenic radionuclides age data for Quaternary deposits on samples collected in the Dillon 30′ x 60′ quadrangle, Montana Bureau of Mines and Geology digital analytical data set.

Granger, D.E., 2014, Cosmogenic nuclide burial dating in archaeology and paleoanthropology: Treatise on geochemistry: Second Edition, v. 14, p. 81–97, https://doi.org/:10.1016/B978-0-08-095975-7.01208-0

Harms, T.A., and Baldwin, J.A., 2023, Paleoproterozoic geology of SW Montana: Implications for the paleogeography of the Wyoming craton and for the consolidation of Laurentia, *in* Whitmeyer, S.J., Williams, M.L., Kellett, D.A., and Tikoff, B., eds., Laurentia: Turning points in the evolution of a continent: Geological Society of America Memoir, v. 220, p. 65–79.

James, H.L., 1990, Precambrian geology and bedded iron deposits of the southwestern Ruby Range, Montana, with a section on the Kelly iron deposit of the northeastern Ruby Range: U.S. Geological Survey Professional Paper 1495, 39 p., 2 plates, scale 1:4,600 and 1:24,000.

James, H.L., and Hedge, C.E., 1980, Age of the basement rocks of southwest Montana: Geological Society of America Bulletin, v. 91, p. 11–15.

Jones, C.L., 2008, U-Pb geochronology of monazite and zircon in Precambrian metamorphic rocks from the Ruby Range, SW Montana: Deciphering geological events that shaped the NW Wyoming province: Kent, Ohio, Kent State University, M.S. thesis, 119 p.

Karasevich, L.P., 1980, Structure of the Pre-Beltian metamorphic rocks of the northern Ruby Range, southwestern Montana: State College, Penn., Penn State University, M.S. thesis, 172 p., 2 plates, scale 1:24,000.

Karasevich, L.P., Garihan, J.M., Dahl, P.S., and Okuma, A.F., 1981, Summary of Precambrian metamorphic and structural history, Ruby Range, Southwest Montana, *in* Tucker, T.E., ed., 1981 Montana Geological Society Field Conference and Symposium to Southwest Montana, v. 26, p. 225–238.

Le Bas, M.J., Le Maitre, R.W., Streckeisen, A., and Zanettin, B., 1986, IUGS Subcommission on the systematics of igneous rocks, a chemical classification of volcanic rocks based on the total alkali-silica diagram: Journal of Petrology, v. 27, no. 3, p. 745–750, https://doi.org/10.1093/petrology/27.3.745

Link, P.K., Todt, M.K., Pearson, D.M., and Thomas, R.C., 2017, 500–490 Ma detrital zircons in Upper Cambrian Worm Creek and correlative sandstones, Idaho, Montana, and Wyoming: Magmatism and tectonism within the passive margin: Lithosphere, v. 9, no. 6, p. 910–926.

Ludwig, K.R., 2012, Isoplot, a geochronological toolkit for Microsoft Excel: Berkeley Geochronology Center, Special Publication 5, 75 p.

Mosolf, J.G., in review, Geologic map of the Bannack 7.5′ quadrangle, Beaverhead County, Montana: Montana Bureau of Mines and Geology Geologic Map.

Mosolf, J.G., Brennan, D., and Kylander-Clark, A., 2023a, U-Pb geochronology data from rock samples collected in the Dillon, Ennis, Gardiner, Hamilton, Hebgen Lake, and Wisdom 30′ x 60′ quadrangles, western Montana, 2022–2023: Montana Bureau of Mines and Geology Analytical Dataset 3.

Mosolf, J.G., Brennan, D., Gavillot, Y., Parker, S., and Sears, J., 2023b, Major oxide and trace element analyses of rock samples collected in the Dillon and Hamilton 30′ x 60′ quadrangles, southwest Montana: Montana Bureau of Mines and Geology Analytical Dataset 2.

Parker, S.D., and Gavillot, Y.G., 2024, Geologic map of the Laurin Canyon 7.5′ quadrangle, Madison County, Montana: Montana Bureau of Mines and Geology Geologic Map 98, 1 sheet, scale 1:24,000. https://doi.org/10.59691/WMJR3264

Ruppel, E.T., O'Neill, J.M., and Lopez, D.A., 1983, Preliminary geologic map of the Dillon 1° x 2° quadrangle, Montana: U.S. Geological Survey Open-File Report 83-168, scale 1:250,000.

Ruppel, E.T., O'Neill, J.M., and Lopez, D.A., 1993, Geologic map of the Dillon 1° x 2° quadrangle, Idaho and Montana: U.S. Geological Survey Miscellaneous Investigations Series Map I-1803-H, scale 1:250,000.

Sales, J.K., 1983, Collapse of Rocky Mountain basement uplifts, *in* Lowell, J.D., ed., Rocky Mountain foreland basins and uplifts: Rocky Mountain Association of Geologists, p. 79–97.

Sandberg, C.A., 1965, Nomenclature and correlation of lithologic subdivisions of the Jefferson and Three Forks formations of southern Montana and northern Wyoming: U.S. Geological Survey Bulletin 1194-N, 18 p.

Sando, W.J., and Dutro, J.T., 1974, Type sections of the Madison Group (Mississippian) and its subdivisions in Montana: U.S. Geological Survey Professional Paper 842, 22 p., 1 plate.

Sando, W.J., and Sandberg, C.A., 1985, Revision of Mississippian stratigraphy, Northern Tendoy Mountains, southwest Montana: U.S. Geological Survey Bulletin 1656, p. A1–A9.

Schmidt, C.J., and Garihan, J.M., 1983, Laramide tectonic development of the Rocky Mountain foreland of Southwestern Montana, *in* Lowell, J.D., ed., Rocky Mountain foreland basins and uplifts: Rocky Mountain Association of Geologists, p. 271–294.

Schmidt, C.J., O'Neill, J.M., and Brandon, W.C., 1988, Influence of Rocky Mountain foreland uplifts on the development of the frontal fold and thrust belt, southwestern Montana, *in* Schmidt, C.J., and Perry, W.J., eds., Interaction of the Rocky Mountain foreland and the Cordilleran thrust belt: Geological Society of America Memoirs, v. 17, p. 171–202.

Stickney, M.C., 2022, Earthquakes and seismographic monitoring in Montana, *in* Metesh, J. and Gammons, C.H., eds., Geology of Montana: Montana Bureau of Mines and Geology Special Publication 122, http://www.mbmg.mtech.edu/pubs/GeologyofMontana, digital only.

Stickney, M.C., Haller, K.M., and Machette, M.N., 2000, Quaternary faults and seismicity in Western Montana: Montana Bureau of Mines and Geology Special Publication 114, 1 sheet, scale 1:750,000.

Stotter, S.V., 2019, Determining the Precambrian structure and thermotectonic evolution of the central Ruby Range, southwest Montana: Missoula, University of Montana, M.S. thesis, 78 p., 1 plate, scale 1:24,000.

Thomas, R.C., 2007, A field guide to the Cambrian section at Camp Creek, southwest Montana: Northwest Geology, v. 36, p. 231–244.

Tysdal, R.G., 1970, Geology of the north end of the Ruby Range, southwestern Montana: Missoula, University of Montana, Ph.D. dissertation, 187 p., 6 plates, scale 1:24,000.

Tysdal, R.G., 1976, Geologic map of the northern part of Ruby Range, Madison County, Montana: U.S. Geological Survey Miscellaneous Investigations Series Map I-951, scale 1:24,000.

Tysdal, R.G., 1981, Foreland deformation in the northern part of the Ruby Range of Southwest Montana, *in* Tucker, T.E., ed., 1981 Montana Geological Society Field Conference and Symposium to Southwest Montana, v. 26, p. 215–224.

Tysdal, R.G., Lee, G.K., Hassemer, J.H., Hanna, W.F., Schmauch, S.W., and Berg, R.B., 1987, Mineral resources of the Ruby Mountains Wilderness Study Area, Madison County, Montana: U.S. Geological Survey Bulletin 1724, 22 p., 1 plate, scale 1:24,000.

Vuke, S.M., Porter, K.W., Lonn, J.D., and Lopez, D.A., 2007, Geologic map of Montana: Montana Bureau of Mines and Geology Geologic Map 62-A, 73 p., 2 sheets, scale 1:500,000.

Wardlaw, B.R., and Pecora, W.C., 1985, New Mississippian-Pennsylvanian stratigraphic units in southwest Montana and adjacent Idaho: U.S. Geological Survey Bulletin 1656, p. B1–B9.

Wilson, M.L., 1981, Origin of Archean lithologies in the southern Tobacco Root and northern Ruby Ranges of southwestern Montana, *in* Tucker, T.E., ed., 1981 Montana Geological Society Field Conference and Symposium to Southwest Montana, v. 26, p. 37–43.

Wooden, J.L., Vitaliano, C.J., Koehler, S.W., and Ragland, P.C., 1978, The late Precambrian mafic dikes of the southern Tobacco Root Mountains, Montana: Geochemistry, Rb-Sr geochronology and relationship to Belt tectonics: Canadian Journal of Earth Science, v. 15, p. 467–479.

Geologic Map 101

Geologic Map of the Beaverhead Rock SE 7.5′ Quadrangle, Madison County, Montana

Yann G. Gavillot, Stuart D. Parker, and Dave M. Pearson

2024

https://doi.org/10.59691/AKIR4686

Research supported by the U.S. Geological Survey, National Cooperative Geologic Mapping Program, under USGS award G22AC00376.
GIS production: Yann Gavillot, Stuart Parker, and Trish Ekberg, MBMG. Map layout: Susan Smith, MBMG. Editing: Susan Barth, MBMG.